

Supporting Information for

Formation of the tetranuclear, tetrakis-terminal-imido $\text{Mn}^{\text{IV}}_4(\text{N}^t\text{Bu})_8$ cubane cluster by four-electron reductive elimination of $^t\text{BuN}=\text{N}^t\text{Bu}$. The role of the s-block ion in stabilization of high-oxidation state intermediates.

**Shivaiah Vaddypally, Sandeep K. Kondaveeti, John H. Roudebush,
Robert J. Cava and Michael J. Zdilla**

Table of Contents

Experimental	3
NMR Spectra.....	5
UV-Vis.....	7
Mass Spectra.....	8
Infrared spectroscopy.....	9
Bond Valence Summation calculations.....	10
Magnetometry.....	11
X-ray crystallography.....	12

Experimental

General Methods:

All manipulations were performed under a rigorous dry, anaerobic atmosphere of nitrogen or argon gas using standard Glove Box and Schlenk line techniques. All reagents were purchased from commercial sources (Aldrich, Strem). Anhydrous solvents were used throughout all experiments. Anhydrous benzene, acetonitrile and pentane were purified using an Innovative Technology, Inc. Pure Solv.TM system. Tetrahydrofuran and hexamethyldisiloxane were distilled from sodium benzophenone ketyl under a nitrogen atmosphere. $\text{Li}_3\text{Mn}_4\text{M}(\text{Bu})_{10}(\text{N})$ ($\text{M} = \text{Mn}\equiv\text{N}/\text{Li}$, **1/1a**) was prepared as previously described.¹¹

X-ray diffraction data were collected on a Bruker KAPPA APEX II DUO diffractometer using Mo-K α radiation from a sealed Mo tube with a TRIUMPH monochromator, equipped with an Oxford Cryostream variable temperature system. Data was collected at -173 °C. Data were integrated, scaled with application of multi-scan absorption correction, solved using direct methods, and refined using full-matrix least squares (SHELXTL). ¹H-NMR spectra were recorded on a Bruker Advance 400 MHz spectrometer with spectral width of 200 ppm. Values for chemical shifts (ppm) are referenced to the residual protiosolvent resonances (C_6D_6 7.16 ppm). FT-IR measurements were performed using a Nicolet Varian Cary 380 FT-IR under nitrogen atmosphere using a KBr pellet press. UV-visible spectra were recorded on a Shimadzu UV-2550 UV spectrophotometer in the range of 200-900 nm. High resolution electrospray ionization mass spectroscopic analyses were performed on a JEOL AccuTof fitted with an electrospray source. LC/MS was performed on an Agilent 6520 Q-TOF ESI mass spectrometer. Cyclic voltammograms were obtained using a CHI-630D electrochemical analyzer/workstation with Picoamp booster. Electrochemical studies were performed under anaerobic conditions using 7 mg **2** in 5 mL of 1:1 acetonitrile:tetrahydrofuran solvent with *tert*-butyl ammonium perchlorate electrolyte (0.1 M) using a standard three-electrode assembly; glassy Pt working, Pt wire auxiliary, and a Ag/AgClO₄ (0.01 M) reference were employed. Potentials were corrected to ferrocene, which was used as an internal standard. Microanalysis data were obtained from the CENTC Elemental Analysis Facility at the University of Rochester. Samples were weighed with a PerkinElmer Model AD-6 Autobalance and their compositions were determined with a PerkinElmer 2400 Series II Analyzer. Air-sensitive samples were handled in a VAC Atmospheres glovebox. Solid state magnetic measurements were carried out on a Quantum Design Model 6000 Physical Property Measurement System. NMR data were fitted to Lorentzian curves using Kaleidograph 4.1.0.

Mn₄(μ_3 -N'Bu)₄(N'Bu)₄ (2**).** In a pressure flask, 0.358g (0.363 mmol assuming a 1:4 mixture of **1:1a**) of **1/1a** was dissolved in 20 mL 1:1 tetrahydrofuran:acetonitrile. To this was added excess (~0.6 g) Et₄NCl). This reaction is heated to 120 °C in an oil bath and stirred for 24 h, resulting in a dark brown mixture. The solution is cooled to room temperature, filtered to remove the solid, and the filtrate is dried under vacuum. The dried filtrate is extracted for 1 h in 20 mL of pentane, filtered, and the solution placed into a

double vial apparatus for vapor diffusion with an excess of hexamethyldisiloxane (HMDS) in the outer jar. These solvents are permitted to diffuse at room temperature for 3-4 days, resulting in large black crystals of **2** in a black mother liquor, which is decanted away using a disposable pipette. The crystalline material is *briefly* rinsed with a minimum of cold (-30° C) pentane, which is decanted quickly before warming up. This leaves 0.094 g (0.12 mmol, 33%) of crystalline **2**, which is dried in vacuo. Due to the hypersolubility of **2**, the final product is frequently contaminated by approximately up to 5% grease, oil, and a small amount of unidentified diamagnetic compound. By further pentane rinses, the purity can normally be improved, but at the expense of yield. ¹H NMR [ppm] (400 MHz, C₆D₆): δ 1.465 (s, ^tBu), 1.712 (s, ^tBu). UV-Vis (C₆H₆): λ_{max} [nm] (ε) 300 (3400), 446 (610), 566 (410), 698 (450). FT-IR: [cm⁻¹] 2970, 2920, 2870 (C-H stretch); 1450, 1380, 1350 (C-H bend) 1220 (M=NR stretch). ESI MS [m/z] (m/z theory): Mn₄(N^tBu)₅(NH^tBu)₂(MeCN)⁺ 760.298 (760.309). CHN Analysis Calcd for C₃₂H₇₂Mn₄N₈: C, 48.71; H, 9.20; N, 14.21. Found: C, 47.89; H, 8.97; N, 14.63.

Identification of azo-*tert*-butane byproduct.

The synthesis of **2** is carried out as described above, except that the solvent is vacuum distilled into a liquid N₂ trap to quantitatively trap the volatiles. This solution is analyzed by LC/MS, which identifies ^tBuN=N^tBu as the only detected organic byproduct of the reaction. The result is shown in figure S6.

Determination of yield of **2** in situ.

Reaction of **1** (27 mg, 0.028 mmol) with excess Et₄NCl (~100 mg) was carried out according to the general protocol for the synthesis of **2**. The pentane extract was dried, redissolved in benzene-*d*₆ and 5 μL of toluene (0.047 mmol) was added as an internal standard. The solution was analyzed by ¹H NMR. Comparison of the integral of the peak for **2** at 1.46 ppm (36 H) to the methyl signal of toluene at 2.11 ppm (3 H) gave a ratio of 0.57 to 1, indicated a yield of 0.022 mmol (81%). The result is shown in figure S3.

Determination of yield of azo-*tert*-butane in situ.

The reaction for synthesis of compound **2** was prepared in situ using the conditions described above for the synthesis of **2**. Compound **1** (24 mg, 0.025 mmol) was reacted with excess Et₄NCl (~ 100 mg) in 1:1 tetrahydrofuran-*d*₈:acetonitrile-*d*₃. After being cooled, the solution was analyzed by ¹H NMR, then spiked with 10 μL (0.053 mmol) azo-*tert*-butane, and reanalyzed by ¹H NMR. Due to the overlap of the azo-*tert*-butane signal with the THF resonance, the signals were integrated by fitting the NMR spectra to Lorentzian curves. Based upon this analysis, the azo-*tert*-butane signal grew by 3.6 times, indicating the product yield from the reaction to be 0.015 mmol (0.018 mmol theoretical yield based on eq. 2, 80% yield). The result is shown in figure S2

NMR spectra.

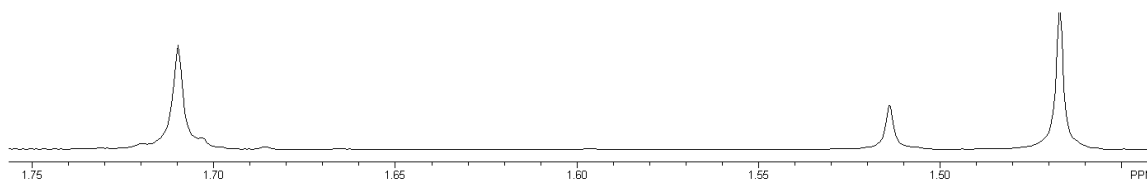


Figure S1. ¹H NMR spectrum of **2**, illustrating the two dominant signals for **2** at 1.47 and 1.71.

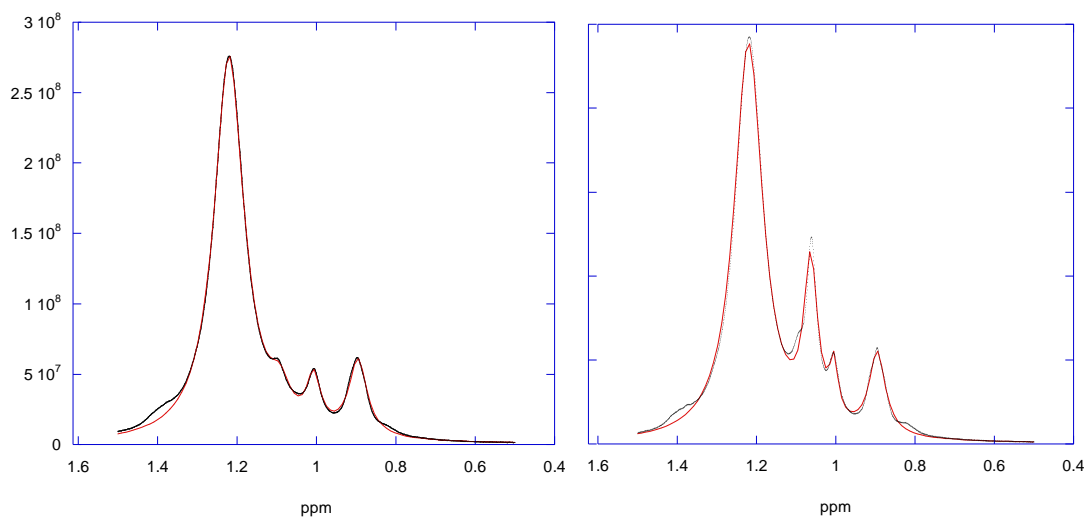


Figure S2: Fitting of ¹H NMR spectra for the determination of azo-*tert*-butane yield (see experimental section). Data are shown in black points and theoretical fits using four Lorentzian curves are shown in red. Left: spectrum after reaction; right: after spiking with 10 μL azo-*tert*-butane. The integral for the signal at 1.1 ppm grows by 3.6 x after the addition of standard.

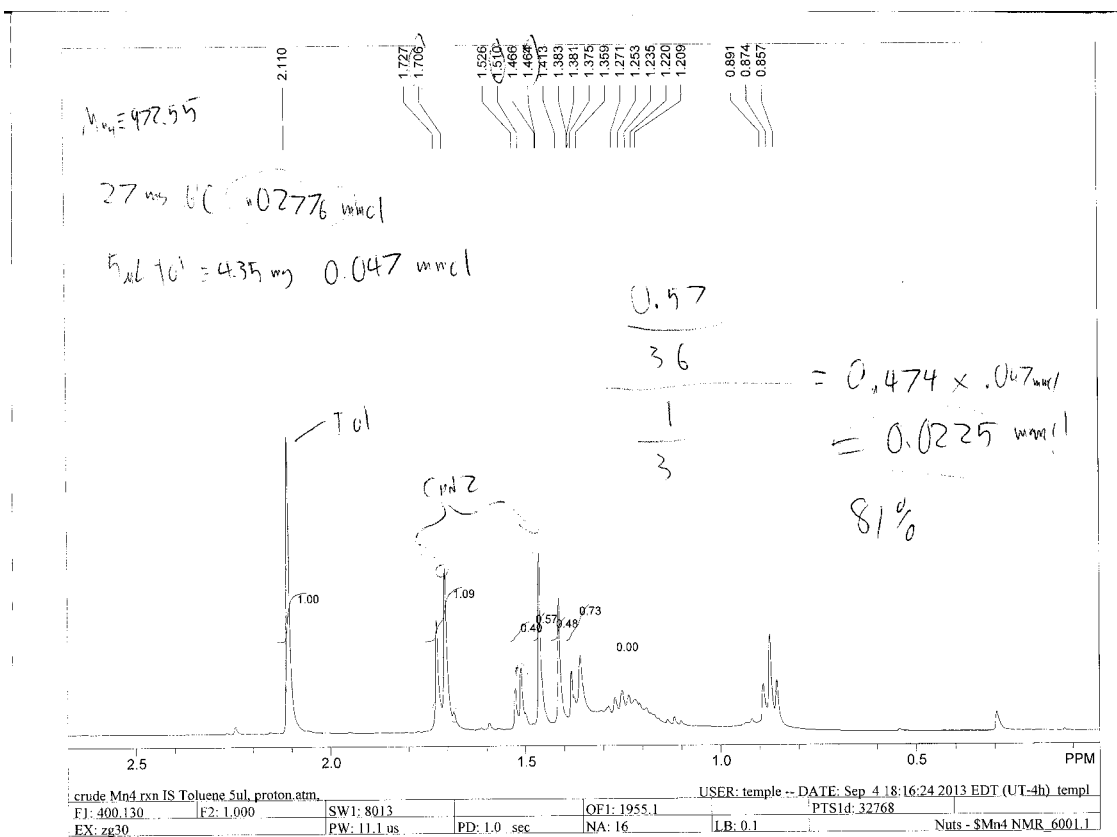


Figure S3. In situ quantification of **2** by comparison of peak integral to toluene internal standard (see experimental section).

UV-Visible spectrum

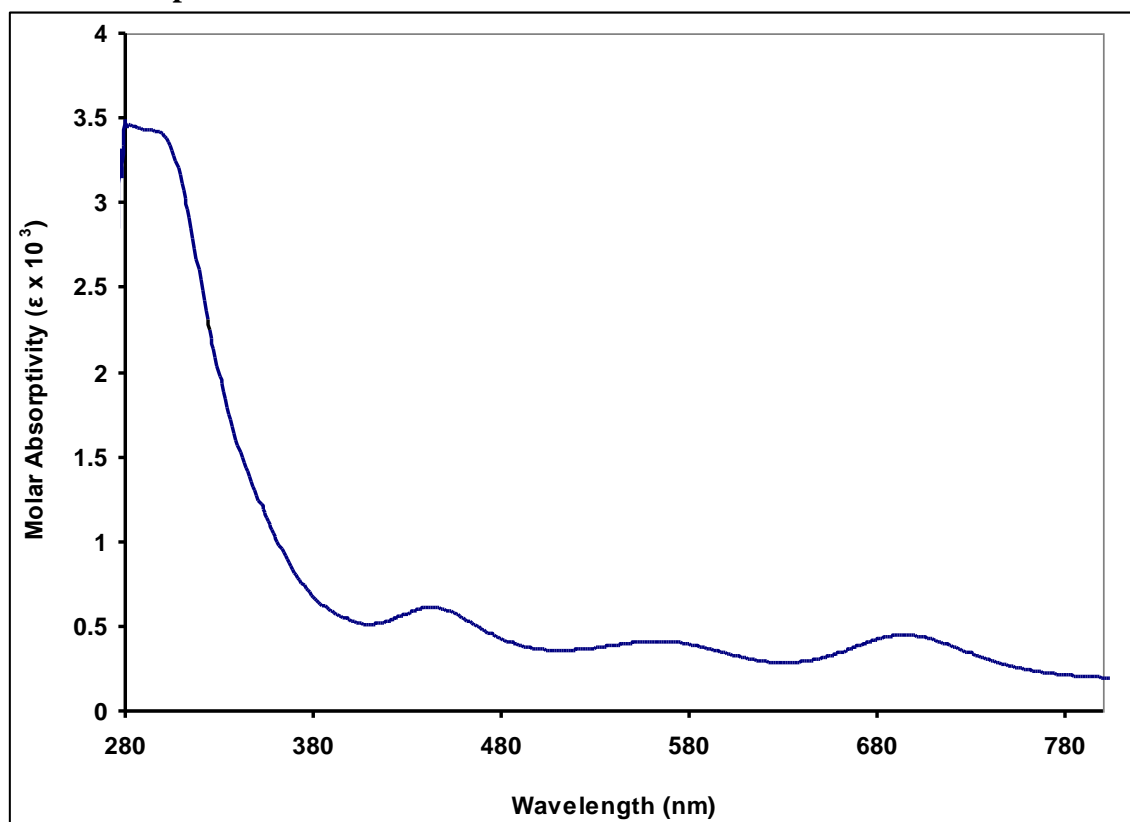


Figure S4. UV-Visible Absorption spectrum of $\text{Mn}_4(\text{N}^t\text{Bu})_8$ (**2**)

Mass Spectra

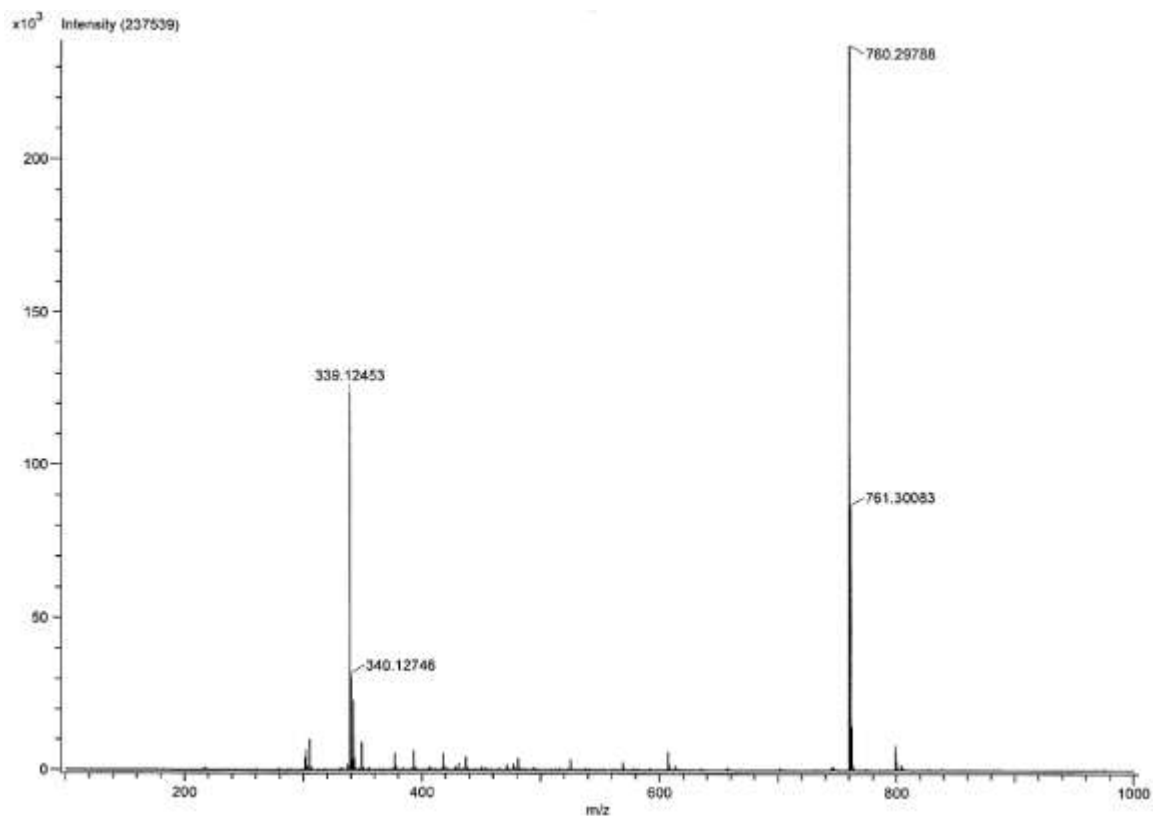


Figure S5. Mass spectrum of **2** detected as protonated acetonitrile ligate $\text{Mn}_4(\text{N}^t\text{Bu})_5(\text{NH}^t\text{Bu})_2(\text{MeCN})^+$

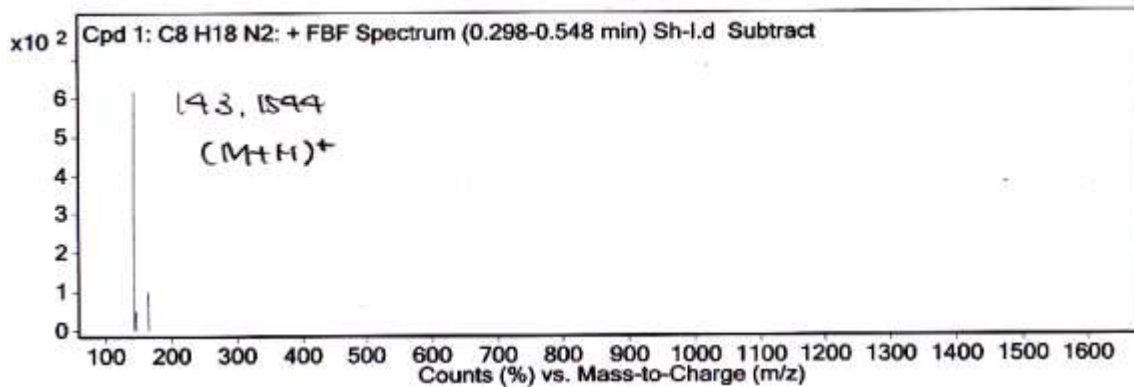


Figure S6. Mass spectrum of product azo-*tert*-butane formed in formation of **2**.

Infrared spectrum

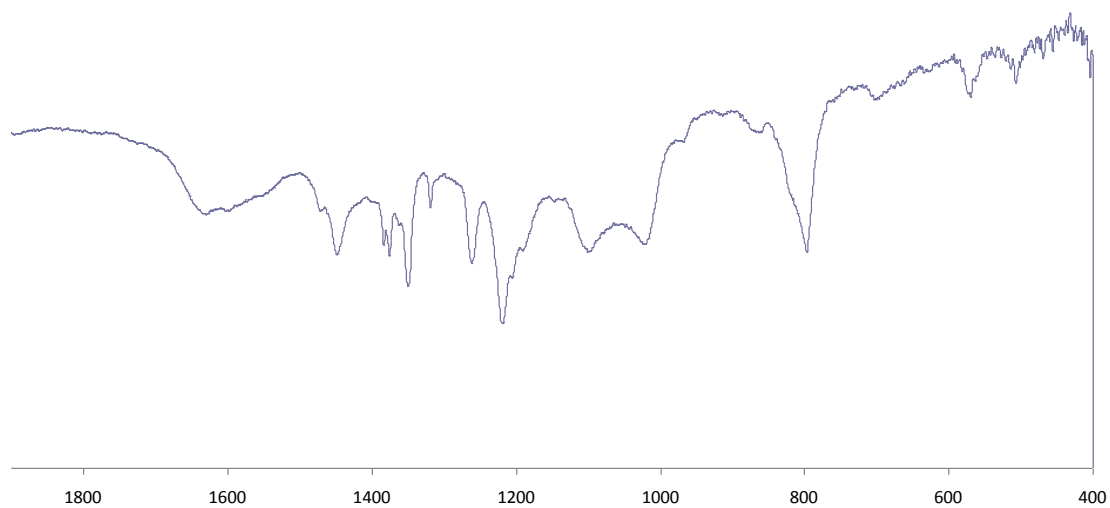


Figure S7. FTIR spectrum of **2** in a KBr Pellet.

Bond Valence Summation Calculations

Bond valence calculation. Numbers in brackets
after atom symbols are at.no., r and c -
see O'Keefe and Brese, J.A.C.S. 1991, 113, 3226

Mn1

Mn (25, 1.17, 1.60)		Rij	Dij	Vij
-N (7, .72, 2.61)		1.86	1.65	1.79
-N (7, .72, 2.61)		1.86	1.91	.88
-N (7, .72, 2.61)		1.86	1.89	.93
-N (7, .72, 2.61)		1.86	1.91	.89

Bond valence sum for Mn 4.48

Mn2

Mn (25, 1.17, 1.60)		Rij	Dij	Vij
-N (7, .72, 2.61)		1.86	1.90	.90
-N (7, .72, 2.61)		1.86	1.91	.87
-N (7, .72, 2.61)		1.86	1.91	.87
-N (7, .72, 2.61)		1.86	1.65	1.79

Bond valence sum for Mn 4.43

Mn3

Mn (25, 1.17, 1.60)		Rij	Dij	Vij
-N (7, .72, 2.61)		1.86	1.89	.94
-N (7, .72, 2.61)		1.86	1.65	1.78
-N (7, .72, 2.61)		1.86	1.89	.94
-N (7, .72, 2.61)		1.86	1.90	.90

Bond valence sum for Mn 4.55

Mn4

Mn (25, 1.17, 1.60)		Rij	Dij	Vij
-N (7, .72, 2.61)		1.86	1.65	1.79
-N (7, .72, 2.61)		1.86	1.91	.88
-N (7, .72, 2.61)		1.86	1.89	.93
-N (7, .72, 2.61)		1.86	1.91	.89

Bond valence sum for Mn 4.48

Magnetic Measurements

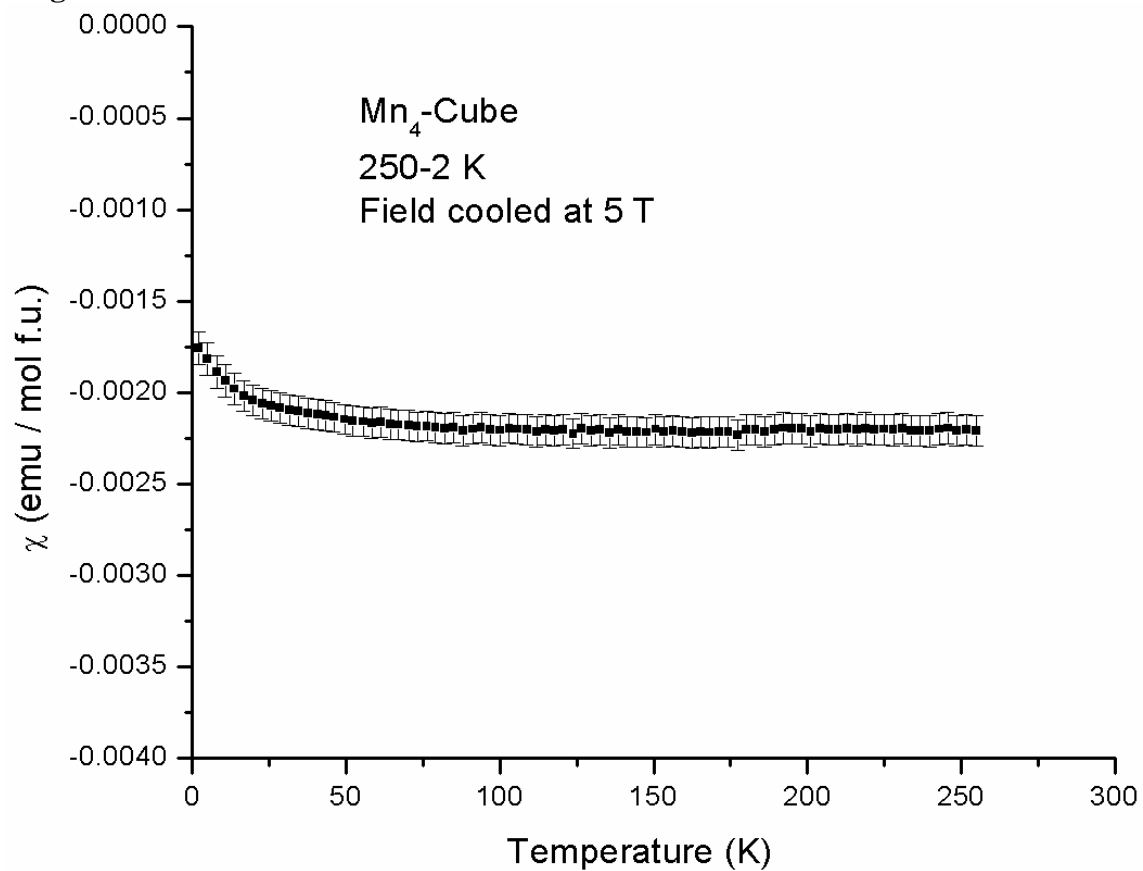


Figure S8. Magnetic measurements on complex **2** showing classic diamagnetic behavior.

X-ray crystallography

A dark black block-like specimen of $C_{32}H_{72}Mn_4N_8$, approximate dimensions 0.070 mm x 0.260 mm x 0.400 mm, was used for the X-ray crystallographic analysis. The X-ray intensity data were measured.

The total exposure time was 4.90 hours. The frames were integrated with the Bruker SAINT software package using a narrow-frame algorithm. The integration of the data using an orthorhombic unit cell yielded a total of 7701 reflections to a maximum θ angle of 27.98° (0.76 \AA resolution), of which 3938 were independent (average redundancy 1.956, completeness = 98.2%, $R_{\text{int}} = 2.24\%$) and 3722 (94.51%) were greater than $2\sigma(F^2)$. The final cell constants of $a = 16.636(2) \text{ \AA}$, $b = 12.5912(18) \text{ \AA}$, $c = 19.216(2) \text{ \AA}$, volume = $4025.1(9) \text{ \AA}^3$, are based upon the refinement of the XYZ-centroids of 7903 reflections above $20 \sigma(I)$ with $5.873^\circ < 2\theta < 55.85^\circ$. The calculated minimum and maximum transmission coefficients (based on crystal size) are 0.6332 and 0.9172.

The structure was solved and refined using the Bruker SHELXTL Software Package, using the space group $Cmcc21$, with $Z = 4$ for the formula unit, $C_{32}H_{72}Mn_4N_8$. The final anisotropic full-matrix least-squares refinement on F^2 with 260 variables converged at $R1 = 3.64\%$, for the observed data and $wR2 = 9.22\%$ for all data. The goodness-of-fit was 1.113. The largest peak in the final difference electron density synthesis was $0.650 \text{ e}^-/\text{\AA}^3$ and the largest hole was $-0.626 \text{ e}^-/\text{\AA}^3$ with an RMS deviation of $0.081 \text{ e}^-/\text{\AA}^3$. On the basis of the final model, the calculated density was 1.302 g/cm^3 and $F(000)$, 1680 e^- .

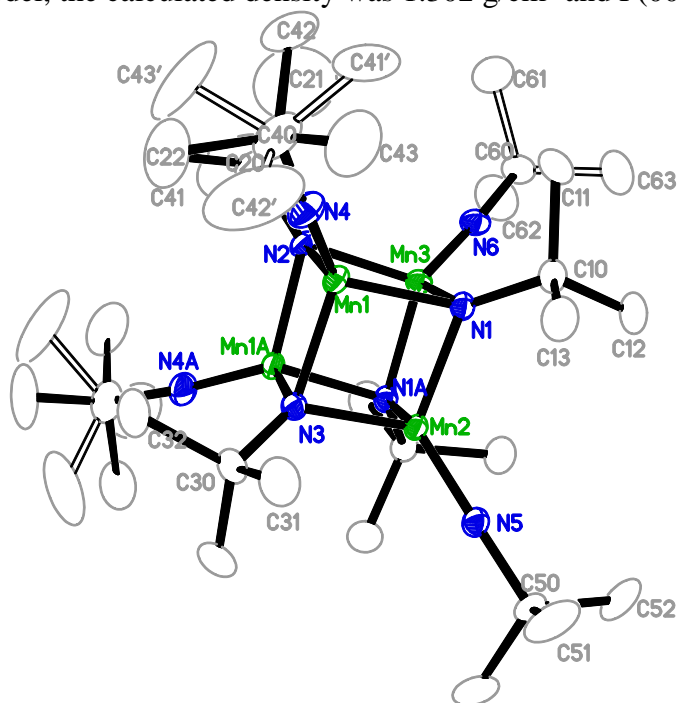


Figure S9. Thermal Ellipsoid plot of $Mn_4(N^tBu)_8$ (**2**). Ellipsoids set at 50% probability level. Carbon atoms shown as open ellipses. Hydrogen atoms omitted for clarity. Symmetry equivalent atoms are generated by the $(2-x, y, z)$ operation.

Table 1. Sample and crystal data for 2.

Chemical formula	$C_{32}H_{72}Mn_4N_8$	
Formula weight	788.73	
Temperature	173(2) K	
Wavelength	0.71073 Å	
Crystal size	0.070 x 0.260 x 0.400 mm	
Crystal habit	dark black block	
Crystal system	orthorhombic	
Space group	C m c 21	
Unit cell dimensions	a = 16.636(2) Å	$\alpha = 90^\circ$
	b = 12.5912(18) Å	$\beta = 90^\circ$
	c = 19.216(2) Å	$\gamma = 90^\circ$
Volume	4025.1(9) Å ³	
Z	4	
Density (calculated)	1.302 g/cm ³	
Absorption coefficient	1.257 mm ⁻¹	
F(000)	1680	

Table 2. Data collection and structure refinement for 2.

Theta range for data collection	2.94 to 27.98°
Index ranges	-16<=h<=21, -11<=k<=16, -25<=l<=25
Reflections collected	7701
Independent reflections	3938 [R(int) = 0.0224]
Coverage of independent reflections	98.2%
Max. and min. transmission	0.9172 and 0.6332
Structure solution technique	direct methods
Structure solution program	SHELXS-2013 (Sheldrick)
Refinement method	Full-matrix least-squares on F ²
Refinement program	SHELXL-2013 (Sheldrick)
Function minimized	$\Sigma w(F_o^2 - F_c^2)^2$
Data / restraints / parameters	3938 / 48 / 260
Goodness-of-fit on F²	1.113
Final R indices	3722 data; R1 = 0.0364, wR2 = 0.0876 I>2σ(I)
	all data R1 = 0.0406, wR2 = 0.0922
Weighting scheme	$w=1/[\sigma^2(F_o^2)+(0.0168P)^2+12.7221P]$ where $P=(F_o^2+2F_c^2)/3$
Absolute structure parameter	0.054(15)
Largest diff. peak and hole	0.650 and -0.626 eÅ ⁻³
R.M.S. deviation from mean	0.081 eÅ ⁻³

Table 3. Bond lengths (Å) for 2.

Mn1-N4	1.644(4)	Mn1-N2	1.892(5)
Mn1-N1	1.905(4)	Mn1-N3	1.909(4)
Mn1-Mn1	2.5364(13)	Mn2-N5	1.649(6)
Mn2-N3	1.901(5)	Mn2-N1	1.913(4)
Mn2-N1	1.913(4)	Mn2-Mn1	2.5606(11)
Mn3-N6	1.651(6)	Mn3-N2	1.886(5)
Mn3-N1	1.899(4)	Mn3-N1	1.899(4)
Mn3-Mn1	2.5395(12)	N1-C10	1.484(6)
N2-C20	1.469(10)	N2-Mn1	1.892(5)
N3-C30	1.479(9)	N3-Mn1	1.909(4)
N4-C40	1.460(6)	N5-C50	1.457(9)
N6-C60	1.446(9)	C10-C12	1.531(7)
C10-C13	1.533(8)	C10-C11	1.537(8)
C20-C21	1.39(2)	C20-C21	1.39(2)
C20-C22	1.442(14)	C30-C31	1.513(8)
C30-C31	1.513(8)	C30-C32	1.559(12)
C40-C41	1.509(9)	C40-C43	1.530(8)
C40-C43'	1.532(12)	C40-C41'	1.534(12)
C40-C42'	1.554(12)	C40-C42	1.566(9)
C50-C52	1.518(12)	C50-C51	1.521(9)
C50-C51	1.521(9)	C60-C62	1.494(9)
C60-C61	1.556(10)	C60-C63	1.556(10)